Electronic Supplementary Information

Enhanced water-responsive actuation of porous *Bombyx mori* silk

Yeojin Jung[ab], Maheen K. Khan[ab], Darjan Podbevšek[b], Tejaswini Sudhakar[c], Raymond S. Tu*[ab], Xi Chen*[abd]

[a] Department of Chemical Engineering, The City College of New York, 160 Convent Avenue, New York, NY 10031, USA
[b] Advanced Science Research Center (ASRC) at the Graduate Center, City University of New York, 85 St. Nicholas Terrace, New York, NY 10031, USA
[c] Department of Biomedical Engineering, The City College of New York, 160 Convent Avenue, New York, NY 10031, USA
[d] Ph.D. Program in Chemistry and Physics, The Graduate Center of the City University of New York, 365 Fifth Avenue, New York, NY 10016, USA
*Corresponding author Email: xchen@gc.cuny.edu; tu@ccny.cuny.edu

Pore Size Analysis of Porous Silk Films

ImageJ was used to analyze the SEM cross section images to characterize pore size. Six smaller equal sized regions of the main image were selected for analysis to reduce the influence of variations in exposure. The images were preprocessed by applying a gaussian blur with radius of 2.00 pixels to reduce noise and were then converted to 8-bit grayscale images. An upper threshold limit on the pixel value, 0 (black) to 255 (white), was manually set by visual inspection to segment the images, capturing the hollow pores in the darkest area and silk skeleton as lightest area. Due to open pore structure of the silk, two different threshold values were used to capture both the smaller discrete pores (pixel value less than about 90), and larger interconnected pores (pixel value less than about 125). The Measure and Analyze Particle functions in ImageJ were used to measure the Feret's diameter, the longest distance between two points along the boundary, of the pores. The results indicate that the porous silk films all have a similar pore size distribution with average diameter of about 40 nm to 50 nm.

Control of air flow

The 6.35 mm-OD poly-vinyl chloride (PVC) tubing (SMC), which allows delivering dry laboratory air and water-saturated air, was connected to a RH chamber to control RH between 10% and 90%. The water-saturated air was generated by passing the lab air through a bubbler connected to an Erlenmeyer flask filled with water. The flow rate of dry and humid air was controlled by solenoid valves (VK332Y, SMC) programmed by LabVIEW. For WR strain and energy density tests, the silk actuator was saturated at 10% and 90% RH for 10 min.

WR speed characterization

The WR speed relaxation time constants (τ) were obtained by fitting the curvature changes of silk/polyimide bilayers over time (t) during hydration and dehydration processes to exponential decay/growth functions [2]:

$$\Gamma(t) = (\Gamma_{Max} - \Gamma_{Min})e^{-t/\tau} + \Gamma_{Min} \tag{S1}$$
$$\Gamma(t) = -(\Gamma_{Max} - \Gamma_{Min})e^{-t/\tau} + \Gamma_{Max} \tag{S2}$$

where Γ is the curvature, Γ_{Max} and Γ_{Min} are the maximum and minimum curvature at 10% and 90% RH, respectively.

Supplementary Figures:

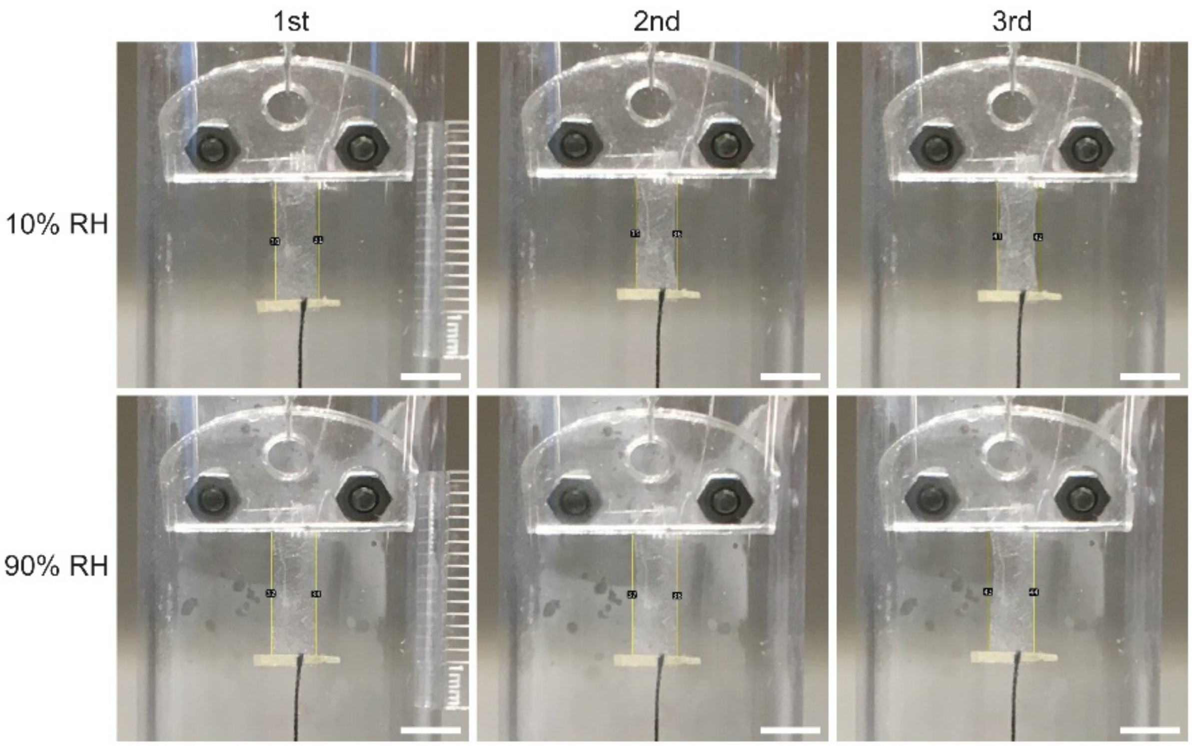

Figure S1. Representative images for WR strain measurement of porous silk films. 10%PEO freestanding films reversibly extend and contract upon RH changes between 10% to 90%. Scale bar, 5 mm.

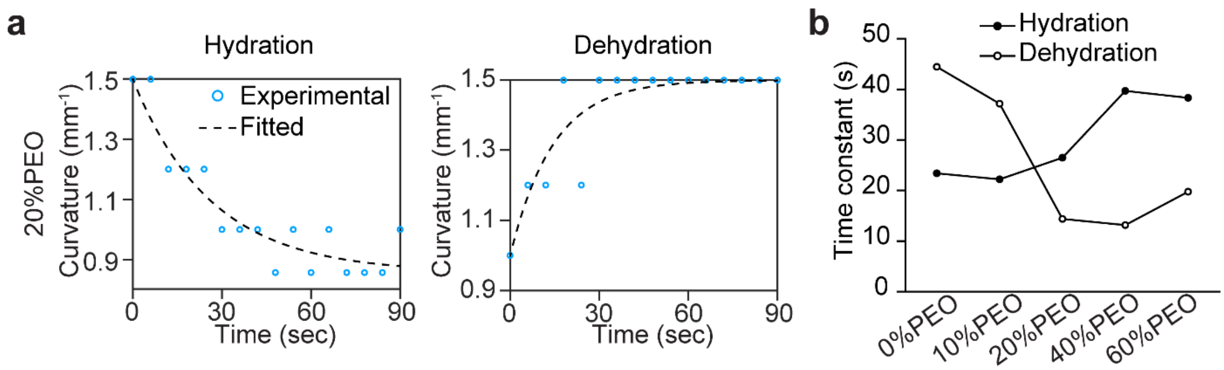

Figure S2. (a) Representative curvature changes over time of silk/polyimide bilayers (20%PEO). (b) Estimated WR speed relaxation time constants of silk/polyimide bilayers.

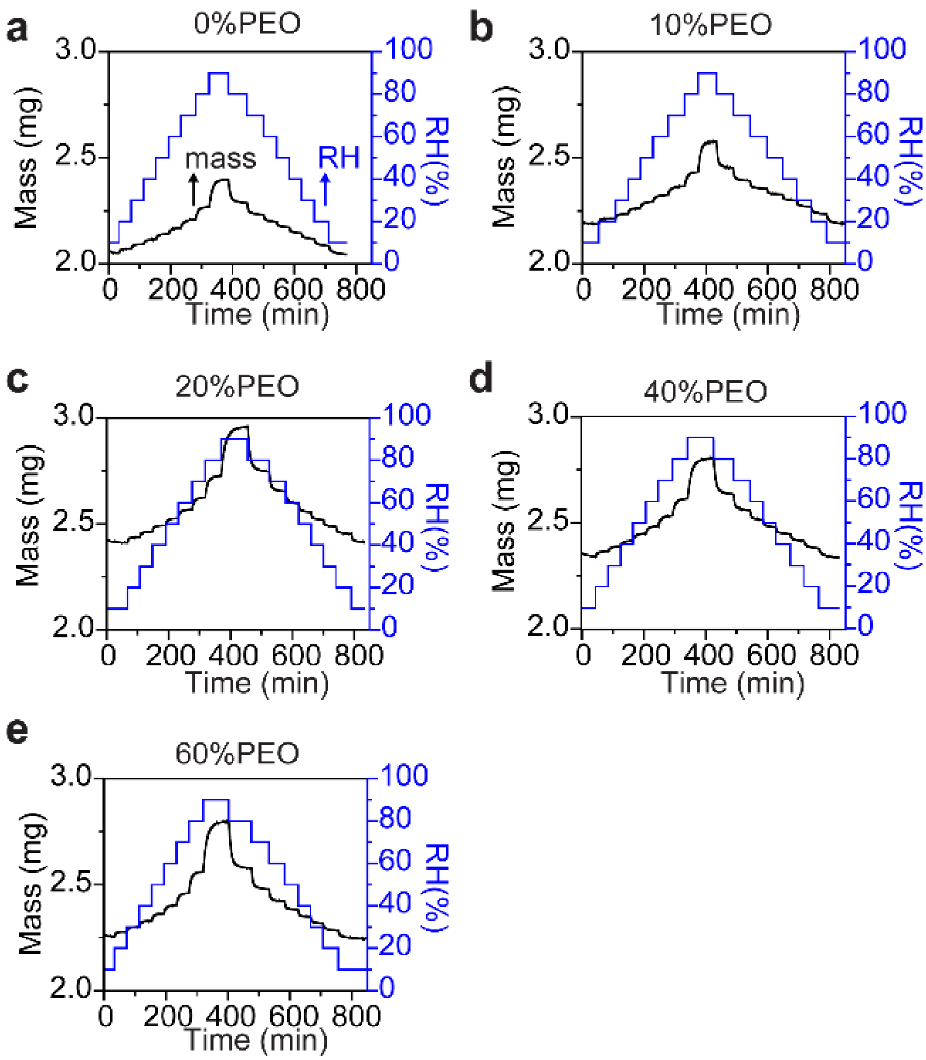

Figure S3. The mass change of porous silk at various RHs during hydration and dehydration processes. (a) 0%PEO, (b) 10%PEO, (c) 20%PEO, (d) 40%PEO, and (e) 60%PEO.

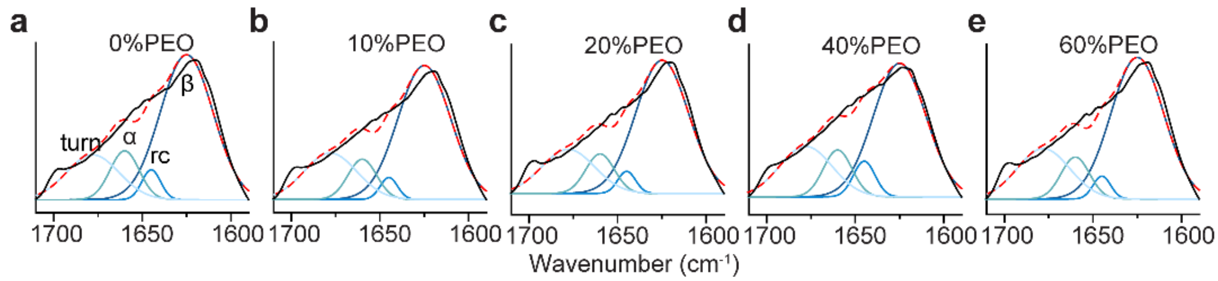

Figure S4. Deconvolution of Amide I bands (1710-1590 cm^{-1}) into 4 sub peaks accounted for β-sheet (1625 cm^{-1}), random coil (1645 cm^{-1}), α-helix (1660 cm^{-1}), and β-turn (1678 cm^{-1}) using Gaussian distribution. Five different spectra were analyzed for each condition. After peak fitting, we assessed our results based on reduced chi square (< 1 ×10^{-6}) and R square (close to 1).

References:

1 H.P. Zhao, X. Q. Feng, H.-J. Shi, *Mater. Sci. Eng. C* **2007**, *27*, 675.

2 H. Wang, Z-L. Liu, J. Lao, S. Zhang, R. Abzalimov, T. Wang and X. Chen, *Adv. Sci.*, **2022**, *9*, 2104697.